This document is the Accepted Manuscript version of a Published Work that appeared in final form in Harmful Algae. To access the final edited and published work see https://doi.org/10.1016/j.hal.2023.102467.

Title: Simulated upwelling and marine heatwave events promote similar growth rates but differential domoic acid toxicity in *Pseudo-nitzschia australis*

Authors: Kyla J. Kelly[a], Amjad Mansour[a], Chen Liang[b], Andrew M. Kim[c], Lily A. Mancini[c], Matthew J. Bertin[c], Bethany D. Jenkins[d,e], David A. Hutchins[a], Fei-Xue Fu[a]*

[a]Marine and Environmental Biology, University of Southern California, Los Angeles, CA, United States

[b]Population and Public Health Sciences, Keck School of Medicine, University of Southern California, Los Angeles, CA, United States

[c]Department of Biomedical and Pharmaceutical Sciences, College of Pharmacy, University of Rhode Island, Narragansett, RI, United States

[d]Department of Cell and Molecular Biology, University of Rhode Island, Narragansett, RI, United States

[e]Graduate School of Oceanography, University of Rhode Island, Narragansett, RI, United States

*corresponding author: ffu@usc.edu, 3616 Trousdale Pkwy, Los Angeles, CA, 90089

[1]**Abbreviations**

[1]**NUEs** nitrogen use efficiencies

CCMs carbon concentrating mechanisms

DA domoic acid

Abstract

Along the west coast of the United States, highly toxic *Pseudo-nitzschia* blooms have been associated with two contrasting regional phenomena: seasonal upwelling and marine heatwaves. While upwelling delivers cool water rich in pCO_2 and an abundance of macronutrients to the upper water column, marine heatwaves instead lead to warmer surface waters, low pCO_2, and reduced nutrient availability. Understanding *Pseudo-nitzschia* dynamics under these two conditions is important for bloom forecasting and coastal management, yet the mechanisms driving toxic bloom formation during contrasting upwelling vs. heatwave conditions remain poorly understood. To gain a better understanding of what drives *Pseudo-nitzschia australis* growth and toxicity during these events, multiple-driver scenario or 'cluster' experiments were conducted using temperature, pCO_2, and nutrient levels reflecting conditions during upwelling (13°C, 900 ppm pCO_2, replete nutrients) and two intensities of marine heatwaves (19°C or 20.5°C, 250 ppm pCO_2, reduced macronutrients). While *P. australis* grew equally well under both heatwave and upwelling conditions, similar to what has been observed in the natural environment, cells were only toxic in the upwelling treatment. We also conducted single-driver experiments to gain a mechanistic understanding of which drivers most impact *P. australis* growth and toxicity. These experiments indicated that nitrogen concentration and N:P ratio were likely the drivers that most influenced domoic acid production, while the impacts of temperature or pCO_2 concentration were less pronounced. Together, these experiments may help to provide both mechanistic and holistic

---

ENSO El Niño-Southern Oscillation

pCO_2 partial pressure of carbon dioxide

PDO Pacific Decadal Oscillation

POC particulate organic carbon

perspectives on toxic *P. australis* blooms in the dynamic and changing coastal ocean, where cells interact simultaneously with multiple altered environmental variables.

Keywords

Harmful diatom blooms, *Pseudo-nitzschia*, domoic acid, upwelling, marine heatwaves, biotoxins

1. Introduction

The biologically-rich California Current System is increasingly impacted by two contrasting extreme phenomena: stronger upwelling events and marine heatwaves. These events differentially impact marine ecosystem function through distinct alteration of the bottom-up controls that influence phytoplankton physiology and community structure. Seasonal upwelling-favorable wind conditions vertically transport cold, carbon dioxide- (CO_2) and nutrient-rich deeper water to the surface, fueling high rates of primary productivity (Chavez and Messié 2009; Gruber et al. 2012; Capone and Hutchins 2013). On the other hand, surface ocean warming during marine heatwaves can enhance stratification, consequentially reducing the availability of inorganic nutrients and carbon available for primary producers (Cheung and Frölicher 2020; Gupta et al. 2020).

Climate change is predicted to amplify the intensity of both of these contrasting coastal processes in the California Current System, which may fundamentally alter the marine environment and conditions for phytoplankton (Du and Peterson 2013; Zhu et al. 2017; Smith et al. 2018; Barth et al. 2020; Trainer et al. 2020). Stronger and more frequent upwelling favorable winds could increase the influx of cold water and nutrients, counteracting the effects of warming and enhanced stratification that accompany rising global temperature (Bakun et al. 2015). These conditions may

favor dense and diverse diatom-dominated phytoplankton communities, as this group thrives with high inputs of nutrients (Lassiter et al. 2006; Du and Peterson 2018). Additionally, ocean acidification is likely to intensify with the increased vertical transport of CO_2-rich bottom waters (Gruber et al. 2012; Hauri et al. 2012; Capone and Hutchins 2013). For some phytoplankton groups, this combined exposure to low-pH upwelled waters and global ocean acidification could exceed physiological tolerances and cause cellular stress (Hurd et al. 2009; Hutchins and Fu 2017). On the other hand, upwelling could supplement the amount of inorganic carbon available for photosynthesis, decreasing cellular energy expenditure on carbon concentrating mechanisms (CCMs), especially in phytoplankton groups with low efficiency CCMs and weak Ribulose-1,5-bisphosphate carboxylase/oxygenase (RuBisCO) affinities for CO_2 (Giordano et al. 2005). Therefore, altered temperature, nutrient concentrations, and inorganic carbon availability with a projected increase in upwelling may impact marine phytoplankton community structure and function (Lassiter et al. 2006; Du and Peterson 2018).

Extreme heat events represent the other face of climate change in this coastal upwelling system. Climate models and meta-analyses have attributed the increased frequency, duration, and intensity (e.g., maximum temperature) of marine heatwaves to anthropogenic climate change (Di Lorenzo and Mantua 2016; Oliver et al. 2018; Laufkötter et al. 2020). This increased heatwave severity (extreme heatwaves) also plays a role in changing conditions that drive phytoplankton community structure and system productivity (Soulié et al. 2022). For instance, during the 2013-2015 “blob” heatwave event in the North Pacific Ocean, surface warming and enhanced stratification caused weaker upwelling that reduced nutrient input and therefore overall primary productivity of the system (Cavole et al. 2016; Yang et al. 2018; Peña et al. 2019). In some regions of the North

Pacific, this combination of warming and upwelling relaxation led to a shift in phytoplankton community composition away from diatoms, and towards a high abundance and diversity of dinoflagellates (Du and Peterson 2018). Lab experiments mimicking the temperature effects of heatwaves on natural communities have also demonstrated shifts to low diversity, dinoflagellate-dominated assemblages (Remy et al. 2017). Furthermore, warm water phytoplankton species can invade normally colder temperate regimes during extended surface ocean warming (Ajani et al. 2020). Additionally, during marine heatwaves CO_2 concentrations may be lower due to thermally-reduced gas solubility or following drawdown by phytoplankton (Murata et al. 2002; Chavez and Messié 2009). Decreased inorganic carbon availability could limit rates of carbon fixation by primary producers, or favor species with strong CCMs (Giordano et al. 2005).

Although upwelling and marine heatwaves differentially alter the environmental conditions in the California Current System that control phytoplankton community structure and function, blooms of the toxic diatom *Pseudo-nitzschia australis* have been associated with both of these climatic extremes. This diatom often produces domoic acid, a potent mammalian and avian neurotoxin, which can be harmful to human health, marine ecosystems, and commercial fisheries (Bates et al. 2018). High abundances of *Pseudo-nitzschia* spp. and domoic acid have frequently been observed during springtime upwelling in the California Current System (Lange et al. 1994; Trainer et al. 2000; Brzezinski and Washburn 2011; Schnetzer, Burton H Jones, et al. 2013; Smith et al. 2018). The correlation of toxic blooms and upwelling has led HAB researchers to categorize *Pseudo-nitzschia* as a cold-water genus that blooms following large, pulsed inputs of nutrients.

In contrast, a marine heatwave in 2015 induced a persistent, highly toxic *Pseudo-nitzschia* bloom of unprecedented size. In the northern portion of the California Current System, several species, including *P. australis, P. fraudulenta*, and *P. pungens* thrived in these warmer, low-nutrient, low-CO_2 conditions, resulting in record concentrations of domoic acid in shellfish and marine mammals (McCabe et al. 2016). Over longer time periods, increased concentrations of domoic acid in the Northern California Current System have been correlated with the warm phases of the El Niño-Southern Oscillation (ENSO) and the Pacific Decadal Oscillation (PDO; McKibben et al. 2017, Sandoval-Belmar et al. 2023). This indicates that in some regions heatwaves (and extreme heatwaves) are another trigger of toxic *Pseudo-nitzschia* bloom formation, in addition to upwelling. The cellular strategies that support the remarkable ability of *P. australis* to bloom under these vastly different environmental conditions remain unknown. However, it should be noted that other studies have found little association between heatwaves and *Pseudo-nitzschia* blooms in the Southern California Current system, thus considerations of regional differences are important (Barron et al. 2013; Ryan et al. 2017).

The physiological responses of *P. australis* to single environmental drivers have been well documented (reviewed in Lelong et al. 2012; Trainer et al. 2012; Bates et al. 2018). For instance, warming can increase the growth rate and toxicity of several species of *Pseudo-nitzschia* (Lewis et al. 1993; Zhu et al. 2017). However, one study measured more domoic acid per cell in *P. seriata* at 4°C, compared to cells grown at 15°C (Lundholm et al. 1994). Furthermore, in the absence of other triggering factors such as nutrient limitation, decreases in pH associated with increases in pCO_2 did not themselves greatly alter the amount of total domoic acid produced by *P. multiseries* and *P. fraudulenta* (Sun et al. 2011; Tatters et al. 2012). However, more domoic acid per *Pseudo-*

nitzschia spp. cell was measured in a natural phytoplankton community exposed to 800 ppm pCO_2, relative to 380 ppm (Tatters et al. 2018). Furthermore, growth phase plays an important role, as more domoic acid per *P. australis* cell was measured at higher pCO_2 concentrations in early stationary phase, but not during exponential growth (Wingert and Cochlan, 2021). Lastly, phosphate and silicate limitation have been implicated in increasing both dissolved and cellular domoic acid (Pan et al. 1998; Sun et al. 2011; Tatters et al. 2012). However, sufficient quantities of nitrogen are necessary for domoic acid biosynthesis, as the amino acid glutamate is a building block in its biosynthesis (Bates et al. 1991).

Despite this extensive body of knowledge about the individual impacts of temperature, pCO_2, and nutrients on *Pseudo-nitzschia* spp., little is known about the synergistic effects between multiple variables that may contribute to toxic bloom formation during upwelling and marine heatwaves. Previous multiple-driver studies with *Pseudo-nitzschia* spp. have demonstrated synergistic effects between multiple variables that can exacerbate growth and/or toxicity (Sun et al. 2011; Tatters et al. 2012; Kelly et al. 2021). This suggests that single stressor experiments cannot fully elucidate bloom dynamics in the natural environment where multiple drivers are at play; however, these single stressor experiments are critical to understanding the mechanisms driving observed responses to multiple drivers. To our knowledge, multiple driver experiments have not been used to directly compare the impacts of upwelling and marine heatwaves of *P. australis* toxic bloom formation.

The objective of our experiment was to examine the physiological changes that allow *P. australis* to thrive under these disparate conditions. We studied the impacts of simulated upwelling, marine

heatwaves, and extreme marine heatwaves on *P. australis* physiology and toxicity to gain a better understanding of how blooms may be impacted by these events. Our in-depth approach to this question involved (a) examining relevant variables (temperature, pCO_2, and nutrients) clustered together into a scenario approach for a holistic understanding, and (b) single-driver experiments for a mechanistic understanding of how individual variables may be impacting the responses we see. We hypothesized that similar to what has been observed in the field, *P. australis* would be able to grow and produce toxins under both heatwave and upwelling conditions.

2. Materials and Methods

2.1 Culture maintenance

Pseudo-nitzschia australis (strain NWFSC 731) was isolated from Long Beach, Washington State, USA on November 3, 2020. The temperature and salinity were 14°C and 27 ppt, respectively at the time of collection. In the lab, cultures were maintained in modified *f*/2 medium under 120 µmol photons m^{-2} s^{-1} LED light on a 12:12 light:dark cycle. The salinity of waters off the Washington coast can fluctuate between 19.7 and 33 ppt dependent on riverine input (Aguilar-Islas and Bruland 2006). The salinity of the natural seawater used to make maintenance media was 33 ppt and cultures were maintained at this salinity for all experiments. To make modified *f*/2 medium, natural seawater was collected from the San Pedro Ocean Time Series site (33° 33’ N, 118° 24’ W). The natural seawater was then filter-sterilized (0.2 µm Whatman Polycap 150 TC cartridge filter) and microwaved. A Panasonic Genius Sensor microwave was used to sterilize 2L bottles of seawater for approximately 16 minutes (until boiling began) at 1250 W, mixing halfway through to ensure homogeneity in temperature. The salinity of the natural seawater collected from the California Bight was reduced from 36 to 33 ppt by diluting with microwave sterilized Milli-Q water. Lastly,

178 the sterilized seawater was amended with nutrients (100 μM nitrate, 100 μM silicate, 6 μM
179 phosphate; standard trace metals and vitamins; Guillard and Ryther, 1962; Guillard, 1975). The
180 seawater used in this study was collected at the surface in the summer. The background nutriment
181 concentrations of phosphate and silicate were 0.3 μM and 1.62 μM respectively. Our values were
182 very close to the concentrations (0.2-0.4 μM phosphate; 2-3 μM silicate) at the surface in the study
183 of Caron et al. (2017), who found that the nitrate concentrations in the surface seawater at this site
184 were almost undetectable (<1 μM). Although the nitrate concentration in the seawater was not
185 measured, it can be assumed to be almost zero since our other two nutrient measurements were
186 close to the values in the study of Caron et al. (2017).
187
188 ***2.2 Experimental conditions***
189 In each experiment, cultures were acclimated to the respective conditions (described below and in
190 Tables 1 & 2) for at least eight generations before sampling. All cultures were maintained semi-
191 continuously in 1L polycarbonate bottles with experimental base medium (sterilized natural
192 seawater + standard *f*/2 trace metals and vitamins; Guillard and Ryther, 1962; Guillard, 1975).
193 Culture volume was also maintained at 1L. Nitrate, silicate, and phosphate were added directly
194 into culture flasks after dilution for final concentrations specific to each treatment (Tables 1 & 2).
195 These semi-continuous culturing methods allowed *P. australis* to remain in the exponential phase
196 of growth by diluting with fresh medium every other day. This repetitive reduction in the number
197 of cells not only prevents cultures from ever reaching the stationary phase of growth, which would
198 lead to self-shading and depletion of nutrients and CO_2, but also allows cultures to determine their
199 own growth rates, based on the conditions to which they are exposed (Kelly et al. 2021; Chen and
200 Gao, 2021). The percentage of the total volume replaced was dependent on the biomass increase

over the dilution cycle; cultures were diluted down to approximately the same initial biomass with each dilution (estimated with in vivo fluorescence).

In the cluster experiments, cultures were simultaneously exposed to a combination of temperature, pCO_2, and nutrient concentrations representative of upwelling, heatwave, and extreme heatwave conditions (Table 1). Values were chosen according to nutrient concentrations measured during the blob heatwave (Du et al., 2016; Gentemann et al. 2017; Gómez-Ocampo et al. 2018; Bif et al. 2019; Jiménez-Quiroz et al. 2019) and upwelling events (Feely et al. 2008; Schnetzer et al. 2013; Siedlecki et al. 2016; Messié et al. 2017; Larkin et al. 2020) off the West Coast of the United States. An additional treatment with low temperature, pCO_2, and nutrient concentrations (LTCN), although less environmentally relevant, was included to tease apart the potential interactive effects due to temperature. In order to change the carbonate chemistry of these cluster experiments, commercial pre-mixed gas was gently bubbled directly into cultures. pH measurements were used during the acclimation phase to characterize the carbonate system (*see Carbonate buffer system measurements* and Table 3).

For the thermal gradient response curve, a temperature gradient was established using a thermal block connected to a VWR 1180-S recirculating chiller and a VWR 1130-2S recirculating heater (Qu et al. 2022). Cultures were grown in modified *f*/2 replete medium (100 μM total nitrate, 100 μM silicate, 6 μM phosphate; standard trace metals and vitamins; Guillard and Ryther, 1962; Guillard, 1975) in triplicate 100 mL polystyrene vials at the following temperatures: 8.4, 11.0, 12.5, 14.1, 15.2, 16.6, 17.7, 19.3, 20.2, 22.7°C. For simplification, each temperature was rounded to the nearest whole number when referenced in the text: 8, 11, 12, 14, 15, 17, 18, 19, 20, 23°C.

In the pCO_2 single-factor experiments, all cultures were grown at 19°C with modified *f*/2 replete medium (described above). Triplicate bottles for each treatment were gently bubbled with commercially pre-mixed gas at concentrations of 200 ppm (pre-industrial), 600 ppm (ocean acidification), and 1040 ppm (extreme ocean acidification). The extreme ocean acidification treatment only had two replicates due to an accidental culture loss the day of sampling. pH was measured daily to characterize the carbonate system (*see Carbonate buffer system measurements* and Table 3). The extreme ocean acidification treatment only had two replicates for physiological measurements as the third replicate was lost during final sampling. A replicate was also removed from the pre-industrial pCO_2 DA quota and production measurements due to a sample processing error.

Two-factor nutrient-temperature experiments were conducted to examine interactive effects between temperature and nutrients, as well as the impacts of N:P ratios on growth and domoic acid biosynthesis. Cultures were grown across a matrix of three nitrogen to phosphorus ratios (N:P=5, 10, 50), two temperatures (13 vs. 19°C), and low vs. high total nutrient concentrations (Table 2). Cultures were diluted semi-continuously with experimental base medium (described above). Post-dilution, cultures were directly spiked with nitrate, phosphate, and silicate for final concentrations specific to each treatment (Table 2).

2.3 Sample collection and analysis

2.3.1 Growth rates

Cultures were sampled once fully acclimated to the experimental conditions (as determined by steady-state growth ±10% for at least 8 generations). Fresh medium in 1L polycarbonate bottles was inoculated with approximately 650 cells/mL and incubated under respective experimental conditions for 48 h.

For the single factor temperature and pCO_2 experiments, specific growth rates were calculated using in vivo chlorophyll a fluorescence measurements. Fluorescence at $T_{initial}$ and T_{final} was measured on a Turner Designs 10-AU fluorometer. For all other experiments, growth rates were calculated using extracted chlorophyll a measurements collected at $T_{initial}$ and T_{final} (see *Pigment analysis*). Specific growth rates were calculated using the following equation:

$$\mu = \frac{\ln\left(\frac{N_{Tfinal}}{N_{Tinitial}}\right)}{T_{final} - T_{initial}}$$

where μ is the specific growth rate (per day) and *N* is the in vivo fluorescence or chlorophyll a concentration (for temperature-only; or cluster, nutrient, and pCO_2 experiments, respectively) at $T_{initial}$ and T_{final} (Kling et al. 2021)

2.3.2 Elemental analysis

For particulate organic carbon (POC) and nitrogen measurements, cells were filtered onto pre-combusted glass microfiber (GF/F) filters (500°C for 3 h) and placed in the drying oven at 60°C for at least 48 h. Filters were pelleted in foil capsules for analysis on a Costech 4010 Elemental Analyzer (Fu et al. 2007).

2.3.3 Domoic acid analysis

Samples for particulate domoic acid were filtered onto Supor 0.2 µm 47 mm PES filters and stored in 15 mL centrifuge tubes at -20°C for 1-4 months (Smith et al. 2017, Harðardóttir et al. 2018, Jennings et al. 2020). The filtrate was also collected and frozen in 100 mL amber HDPE bottles for dissolved domoic acid analysis.

For particulate domoic acid analyses, filters were extracted for four hours in 90% methanol and 10% water, vigorously vortexing each hour following the methods described in Wang et al. (2012) where DA recoveries exceeded 90% in cultured phytoplankton samples. Extracts were passed through a 0.2 µm syringe filter directly into a 1.5 mL LC-MS vial for LC-MS/MS analysis on a Prominence UFLC system (Shimadzu, Kyoto, Japan) coupled to a SCIEX 4500 QTRAP mass spectrometer (AB Sciex, Framingham, MA, USA). The mass spectrometry methods followed those of Sterling et al. (2022) with some minor modifications (the eluent was sent to waste during the first 5 min of the run rather than 2 min and the CRM for DA was obtained from the National Research Council of Canada rather than Sigma-Aldrich). The peak of DA eluted at 11.00 min. LC-MS/MS with multiple reaction monitoring (MRM) was employed for detection and quantification. Analysis was carried out in positive mode, and three transitions from the protonated DA molecule were used: *m/z* 312 → 266 (quantitation transition), *m/z* 312 → 248, and *m/z* 312 → 193. Plankton-associated domoic acid was quantified to ng particulate domoic acid L^{-1} of filtered seawater using an external calibration curve created from pure domoic acid standards of increasing concentrations (CRM, National Research Council of Canada), included in each analysis.

One DA sample was removed from analysis in the pre-industrial treatment in the CO_2 single factor experiment, and from the NP=50, high nutrient, 19°C treatment in the N:P ratio experiment, due to a sampling and/or analytical error.

For environmental relevance and to make inferences about trophic transfer of toxins, domoic acid was normalized to cells per L. Domoic acid was normalized also to moles of POC per liter; because *Pseudo-nitzschia spp.* cell size and volume can change with nutrient limitation, normalizing only to cell counts may result in skewed results (Tatters et al. 2012). In the text, discussion of "DA quotas" refers to this POC normalized value, unless otherwise stated.

Dissolved DA was measured from acidified filtered seawater (50 mL, 0.2 µm) passed over a C18 solid phase extraction column and eluted with methanol based on the methods of Wang et al. 2012 with some modification. The eluent was placed directly into a 1.5 mL LC-MS vial and analyzed using the LC-MS method detailed above.

Domoic acid production rates were calculated by multiplying specific growth rates by DA quotas. This value provides an estimate of how toxic a bloom might be, based on the ability of *Pseudo-nitzschia* to increase cell abundances and produce high DA quotas (per mol POC). For instance, if *Pseudo-nitzschia* is present in high abundances but not toxic, the bloom might not have negative ecosystem implications (Kelly et al. 2021).

2.3.4 Chlorophyll a analysis

Samples for chlorophyll a were filtered on GF/F filters and stored in scintillation vials at -20°C for ~24-48 h. Samples were extracted in 6 mL of 90 % acetone at -20°C for 24 h, then analyzed using a Turner 10AU field fluorometer (Welschmeyer 1994; Fu et al. 2007).

2.3.5 Net carbon fixation and elemental use efficiencies

Primary production was determined by measuring the uptake of radiolabeled bicarbonate (Fu et al. 2008). ^{14}C-bicarbonate was added to 45 mL sub-cultures at $T_{24\ h}$ and incubated for 24 h (approximating net carbon fixation) under the respective experimental conditions. After the incubation period, cells were collected on GF/F filters and placed in a scintillation vial containing scintillation cocktail. Samples were stored for 24 h before being read on a Wallac System 1400 liquid scintillation counter. Carbon fixation rates were calculated by converting raw counts of disintegrations per minute to µmol of carbon (based on total activity of the radiolabeled bicarbonate), then normalizing to the incubation time. Dissolved inorganic carbon (DIC) values used in the calculation were adjusted for each treatment based on measured values of DIC (see below). These rate measurements were then normalized to POC. In the cluster experiment, one sample from the extreme heatwave treatment was removed from primary production analyses due to an error made during the assay.

Nitrogen use efficiencies (NUEs) were calculated by normalizing net carbon fixation rates to particulate organic nitrate (mols C fixed hour^{-1} mol N^{-1}; Yang et al. 2022).

2.3.6 Carbonate buffer system measurements

pH measurements were made on a Mettler Toledo SevenCompact pH meter using a three-point calibration curve and total pH scale (Cooley and Yager 2006). Samples for total DIC analysis were collected at T_{final}. Seawater from undisturbed culture bottles was removed with a sterile syringe, ejected into pre-evacuated borosilicate Exetainers, and poisoned with 5% $MgCl_2$. Samples were stored at 4°C until analysis. Total DIC was measured using a Picarro cavity ring-down spectrophotometer according to Subhas et al. (2015). Experimental seawater pCO_2 and total alkalinity were calculated from measured DIC and pH using CO2SYS version 2.1 software (Table 3; Lewis and Wallace, 1998).

2.3.7 Cell counts

For cell count samples, 1 mL of the final experimental culture was preserved with 40 ul glutaraldehyde and stored at 4°C in the dark. Cells were counted on a Olympus BX51 microscope using a Sedgewick Rafter Chamber.

2.3.8 Statistical methods

Multivariate analyses were conducted in R version 1.3.1093 (http://www.r-project.org) using statistical tools in Rallfun-v38 (https://dornsife.usc.edu/labs/rwilcox/software/). For global analyses, percentile bootstrap methods for comparing 20% trimmed means were used to detect significant differences between treatments. t1way was used in the single-factor and cluster experiments, while t3way was used in the nutrient-temperature experiments. To test for significant differences between any two treatments, pairwise analyses using percentile bootstrapping of 20% trimmed means (trimpb2) were conducted. These statistical tools are analogous to ANOVAs and

post-hoc and Welch's t-test pairwise analyses but are more robust as they do not assume normality or homoscedasticity (Wilcox, 2003).

3. Results

3.1 Multiple driver cluster experiments

Specific growth rates were greatest in the heatwave treatment, but only 17% lower in the upwelling treatment (p-value < 0.01), averaging 0.44 and 0.37 day^{-1} (respectively; Figure 1A). In contrast, *P. australis* growth rates in the extreme heatwave treatment were 61% lower than in the heatwave treatment, although these experimental conditions only differed by 1.5°C in temperature. Furthermore, when *P. australis* was grown with lower heatwave concentrations of nutrients and pCO_2, but also at a reduced temperature (i.e., low temperature, CO_2, and nutrients; LTCN), growth rates were not significantly different from those measured in the extreme heatwave treatments.

Dissolved DA (dDA) concentrations were a negligible fraction of the total DA in all treatments (data not shown), likely due to the constant exponential phase growth and regular culture medium dilutions used in our semi-continuous incubations. POC normalized pDA quotas were highest in the upwelling treatment, averaging 0.9 ng DA µmol C^{-1} (Figure 1B). In contrast, toxins were not detected in the heatwave treatment, and pDA concentrations were 93% lower than upwelling values under extreme heatwave conditions. Furthermore, pDA concentrations for the LTCN treatment were 41% lower than upwelling concentrations. Trends in DA quotas were the same when normalized to cell abundance and to volume (mL), with the greatest quotas measured in the upwelling treatment Table 4). DA production rates demonstrated a similar trend, with the highest production rates measured under upwelling conditions (0.33 ng DA µmolC^{-1} day^{-1}) and zero or

near zero for the heatwave and extreme heatwave treatments (Figure 1C). DA production rates in the LTCN treatment were 92% higher than in the extreme heatwave treatment ($p < 0.01$).

Net C-specific primary productivity trends were similar to those observed for growth rates (Figure 2A). The highest rates were measured in upwelling and heatwave treatments (0.012 and 0.013 day^{-1}, respectively), which were not significantly different from one another ($p = 0.221$). Rates for the LTCN and extreme heatwave conditions were 54% lower that the heatwave treatment ($p < 0.01$).

Nitrogen use efficiencies (NUEs) measure how efficiently the cells use their cellular nitrogen quotas to fix carbon under different experimental conditions. NUEs were highest under heatwave conditions and decreased by 17% in the upwelling treatment ($p = 0.028$ Figure 2B). For the LTCN treatment, NUEs were slightly lower than those for the upwelling treatment ($p < 0.01$). Finally, NUEs for the extreme heatwave treatment declined 61% relative to the heatwave treatments ($p < 0.01$).

3.2 Single factor experiments

When temperature alone was considered, the fastest specific growth rates were measured between 14 and 19°C, reaching a maximum of 0.35 day^{-1} at 18°C (t1way p-value <0.01; Figure 3A). At temperatures above 19°C or below 13°C, growth rates declined rapidly. Furthermore, *P. australis* grew extremely slowly (0.02 day^{-1}) and was unable to persist stably at temperatures $\leq$9°C and could not survive when temperatures exceeded 23°C.

Particulate domoic acid cellular quotas (pDA, ng DA µmol C^{-1}) had an inverse relationship with temperature, whereby pDA decreased as temperature increased, except at 8°C where cold-stressed cultures did not produce any detectable toxin (Figure 3B). The R^2 value was 0.88 for a linear regression that excluded the 8°C values, indicating a strong linear relationship between temperature and pDA. The highest concentrations of pDA were measured at 11°C, averaging 3.52 ng DA µmol C^{-1}. Between 13 and 18°C, pDA quotas were slightly lower than the maximum, though similar to each other. Relative to the maximum, pDA declined by 72% with warming to 19°C and 20°C, and no pDA was measured at 23°C. DA production rates (ng DA µmol C^{-1} d^{-1}) were highest and not significantly different from one another between 11 and 18°C, averaging 0.68 ng DA µmolC^{-1} d^{-1} and decreased by 62% to 19°C. At 8 and 23°C, DA production rates were at or near zero (Figure 3C).

In the single factor CO_2 experiment, the highest growth rates were measured in the 600 µatm treatment (Figure 4A). Growth rates were 23% and 11% lower in the 200 and 1040 µatm treatments, although this difference was only significant for the 200 µatm treatment (pairwise p-value < 0.01). On the other hand, cellular DA content was greatest at the extreme ends of the CO_2 concentration gradient (Figure 4B). In the 600 µatm treatment, DA quotas were 66% and 56% lower relative to 200 µatm and 1040 µatm (respectively, p-values <0.01 and 0.021). Lastly, DA production rates followed a trend similar to DA quotas; the lowest rates were observed at 600 µatm, with a 54% and 50% increase compared to 200 and 1040 µatm (although differences were only statistically significant between 200 and 600 µatm; $p < 0.01$).

3.3 N:P ratio experiments

Within each combination of temperature and total nutrient concentration (i.e., low vs. high nutrients), growth rates were greatest for the treatments with an N:P ratio of 50 (Figure 5A). Within each temperature for the N:P=5 and N:P=10 treatments, differences in growth rates between high and low total nutrient treatments were very minor, yet statistically significant (t3way N:P ratio affects p-value = 0.0001).

There were no other significant 2- or 3-way interactive effects between variables for growth rates in this experiment. Furthermore, growth rates increased with both temperature and higher total nutrient concentrations (high nutrient treatments), except for the 19°C high nutrient N:P=50 treatment.

Particulate domoic acid was not detected in the N:P=5 treatments. The most pDA was produced in the N:P=50 treatments, which were 71 to 90% higher than the N:P=10 treatments (t3way single variable N:P ratio effects p-value = 0.0001; Figure 5B). Furthermore, within the N:P=50 treatments lower concentrations of pDA were measured in the treatments with lower total nutrient concentrations (t3way interactive effects between N:P ratio and total nutrient concentration p-value = 0.014). Differences between N:P=10 treatments were minor at 13°C, yet at 19°C the high total nutrient concentration treatment was 96% higher than the treatment with a low total nutrient concentration (t3way interactive effects between all variables p-value = 0.046).

4. Discussion

4.1 Single factor experiments and potential interactions reveal the influence of each environmental variable the cluster experiment

448 The single and dual factor experiments provided a mechanistic understanding of how the drivers
449 examined contributed to the responses in the cluster experiment. We found that the trends observed
450 in the single-factor treatments could not fully explain the results of the multiple-driver
451 experiments. This provides evidence that non-linear, interactive effects may be influencing trends
452 observed in the multivariate scenario experiments.
453
454 ***4.1.1 Growth rates***
455 Other studies have shown that optimal growth temperatures are highly species and strain dependent
456 (Lelong et al. 2012; Bates et al. 2018). The heatwave temperature was within the broad optimal
457 temperature range for growth for this *P. australis* strain, while the upwelling temperature was
458 suboptimal. This aligns with results from the cluster experiment, where growth rates for the
459 heatwave treatment were slightly higher than those in the upwelling cluster, indicating that
460 temperature did influence growth rates in the cluster experiment. However, temperature was only
461 partially responsible for the decreased growth rates in the extreme heatwave treatment, as growth
462 rates declined more than expected from temperature alone.
463
464 On the other hand, pCO_2 alone had only a slight impact on *P. australis* growth rates. However,
465 inorganic carbon concentration did not influence growth rates in the cluster experiments as
466 expected based on the single factor experiment; growth increased slightly with pCO_2 concentration
467 alone, yet growth was higher in the heatwave treatment with less pCO_2. Similar to the trends
468 observed in the present single-factor study with *P. australis*, increases in growth rates have been
469 observed from 200 to 765 ppm for *P. multiseries* and from 220 to 730 ppm for *P. fraudulenta*.
470 However, when *P. multiseries* and *P. fraudulenta* were both exposed to pCO_2 and limited for either

phosphate or silicate, growth rates further declined, suggesting that there were interactive effects between nutrient limitation and pCO_2 concentration (Sun et al. 2011; Tatters et al. 2012). Zhu et al. (2017) also demonstrated that there were interactive effects of pCO_2 and temperature on *P. subcurvata*; growth rates under suboptimal temperature and high pCO_2 conditions were lower than growth rates at optimal temperatures combined with low pCO_2.

Single-factor nutrient experiments were not conducted in the present study, as individual nutrient effects on *Pseudo-nitzschia* growth have been studied extensively. As with many other diatom species, nutrient limitation typically reduces *Pseudo-nitzschia* growth (Fehling et al. 2004; Hagström et al. 2011; Sun et al. 2011; Tatters et al. 2012; Auro and Cochlan 2013). In the nutrient-temperature matrix experiment, growth rates were higher for treatments with higher total nutrient concentrations. However, in the cluster experiments *P. australis* growth rates were slightly higher in the heatwave treatment, despite having lower nutrient concentrations relative to the upwelling treatment. Furthermore, regardless of equal nutrient concentrations in both heatwave treatments, growth rates in the extreme heatwave treatment were lower. This indicates that there was a temperature-nutrient interaction in the cluster experiments (see below).

4.1.2 Domoic acid quotas

Temperature alone had a significant impact on DA quotas in the present study. In contrast to our observation that DA quotas decreased with warming, most published *Pseudo-nitzschia* studies on temperature have observed increases in DA with warming (Lelong, Hégaret, et al. 2012; Thorel et al. 2014; Zhu et al. 2017; Kelly et al. 2021); however, one found that *P. seriata* produced more DA at relatively colder temperatures, similar to observations in the present study (Lundholm et al.

494 1994). Furthermore, *P. australis* has been associated with relatively cold temperatures in
495 Narraganset Bay, RI (Roche et al. 2022). In March 2017, a highly toxic *P. australis* bloom occurred
496 at temperatures ranging from 1 to 5°C in Narraganset Bay, RI (Sterling et al. 2022). The diversity
497 of thermal tolerances documented in the literature demonstrate that different species and strains of
498 *Pseudo-nitzschia* have distinct thermal triggers for toxin production, though the data in the present
499 study indicates that this strain of *P. australis* specializes in being more toxic at colder temperatures.
500
501 Because temperature alone (under nutrient replete conditions) had a strong inverse relationship
502 with DA concentrations in the single factor experiments, it likely contributed to the differences in
503 DA between cluster treatments where more DA was measured in the cold, upwelling treatment
504 compared to the warm, heatwave treatments. However, in the heatwave and extreme heatwave
505 treatments the decrease in DA quotas were greater than expected based on the temperature single
506 factor experiments. Furthermore, it should be noted that in the upwelling treatment and
507 temperature experiment, nitrogen availability was replete and ample to support DA biosynthesis,
508 which may not have been the case in the heatwave and extreme heatwave cluster treatments (the
509 interactive effects are discussed more below).
510
511 Similar to our observation that more DA was measured at the extreme ends of the pCO_2
512 concentration gradient, another strain of *P. australis* was highly toxic at low and extremely high
513 pCO_2 concentrations (371 and 1849 µatm), and only moderately toxic at an intermediate pCO_2
514 concentration (785 µatm; Ayache et al. 2021). In contrast, other strains of *P. australis* have
515 demonstrated decreases in DA along the same pCO_2 gradient described above, or no change in DA
516 across pCO_2 gradients during the exponential phase of growth (Sun et al. 2011; Tatters et al. 2012;

Ayache et al. 2021; Wingert and Cochlan 2021). While there are species and strain differences with regard to pCO_2 concentration, toxicity of the *P. australis* strain used in the present study is more sensitive to changes in CO_2 alone.

Inorganic carbon may have influenced the upwelling cluster DA quotas, as the extreme ocean acidification pCO_2 concentration in the single factor experiment was similar to the concentration used in the upwelling experiment. However, it is likely that pCO_2 alone did not trigger DA biosynthesis in the heatwave and extreme heatwave cluster treatments. Although the pre-industrial pCO_2 level, similar to levels used in the heatwave and extreme heatwave treatments, did trigger DA biosynthesis, very little to no DA was observed in these clusters.

Previous investigations have robustly demonstrated that phosphate and/or silicate limitation trigger DA biosynthesis in toxic strains of *Pseudo-nitzschia* sp. (Pan et al. 1996; Fehling et al. 2004; Sun et al. 2011; Tatters et al. 2012). This suggests that silicate and phosphate limited conditions should have triggered DA biosynthesis in the heatwave and extreme heatwave treatments, yet little to no DA was measured. However, these treatments were also nitrate limited, and sufficient nitrogen is required for synthesis of DA, a nitrogen-containing molecule (Lelong et al. 2012). Therefore, the total amount of nitrogen in these treatments may have strongly negatively impacted DA quotas (see more below).

4.2 Mechanistic studies and potential interactive effects inform dynamics in the cluster experiment

The three drivers interacted in the cluster experiment to alter growth rates more than expected from individual variables or additive effects. We hypothesize that there was a tradeoff between

temperature, nutrients, and carbon dioxide: at cooler temperatures, high nutrients and inorganic carbon offset the growth limitation of low temperature. On the other hand, warming supported higher growth rates, even if limited by nutrients and inorganic carbon. This indicates that there was a synergistic interactive effect between these three variables.

In terms of bloom toxicity, temperature and inorganic carbon may have partially contributed to the increased DA measured in the upwelling cluster. However, it is likely that the main driver of differences in toxicity between treatments was nitrogen. Both the heatwave treatments were supplied with less nitrogen, while the upwelling treatment had ample nitrate, which is necessary for the biosynthesis of DA molecules (Lelong et al. 2012). Therefore, it is possible that the lack of nitrogen in the heatwave and extreme heatwave treatments had an antagonistic effect, inhibiting DA biosynthesis regardless of the CO_2 conditions that may trigger toxin production. Therefore, we surmise that nitrate concentration was a key factor influencing DA production in the cluster experiments.

DA is a specialized metabolite and biosynthesis is an energetically expensive process. Therefore, DA is typically produced when there is sufficient energy for both processes, or when silicate or phosphate availability limit or reduce cell division (Pan et al. 1998). However, this tradeoff does not always seem to be the case in the present study. In the temperature experiment, slower growth rates and high DA quotas at 11°C were associated with high DA production rates, while higher growth rates at slightly warmer temperatures were associated with lower DA quotas yet near equal DA production rates. For the pCO_2 experiments, differences in growth rates were marginal and DA production rates closely followed DA quota trends. In this case, growth rates were decoupled

563 from bloom toxicity. Together, these experiments demonstrate that high biomass does not
564 necessarily indicate high toxicity, and low biomass does not indicate a low threat of DA poisoning.
565 Similarly, observations of high *Pseudo-nitzschia* sp. biomass yet low DA concentrations have been
566 detected in the natural environment (Roche et al., 2022).
567
568 DA concentrations in the cluster treatments can also be examined through the lens of cellular
569 energetics and the tradeoff between growth and toxicity. In addition to the need for sufficient
570 cellular energy, nitrogen is also required for both growth and DA synthesis. This tradeoff between
571 growth and toxicity is not evident in the cluster experiments: upwelling and heatwave treatments
572 grew equally well yet differed in terms of toxicity. Instead, this may be explained by the total
573 amount of nitrogen available in each treatment.
574
575 Considering growth rate results, DA measurements, and previous studies with nitrogen, we
576 hypothesize that the upwelling treatment had more than enough nitrogen for growth, and the excess
577 was shunted to DA biosynthesis. *P. australis* cells in the heatwave and extreme heatwave
578 treatments had less total nitrogen available. In the heatwave treatment, nitrogen did not limit
579 growth, carbon fixation, or NUEs, but there might not have been enough for concurrent DA
580 synthesis. This indicates that the absolute amount of nitrogen plays a role in the tradeoff between
581 growth and toxicity. Additionally, in the extreme heatwave treatment, both growth rates and DA
582 concentrations were reduced. Previous studies have observed declines in growth rates due to
583 warming, concurrent with increases in toxicity, indicating that the energy and nitrogen not used
584 for growth was instead shunted to DA biosynthesis (Zhu et al. 2017). However, for this strain of

585 *P. australis* the low DA quotas in the extreme heatwave treatment may be due to a lack of sufficient
586 nitrogen and a warming-induced reduction in DA biosynthesis.
587
588 The LTCN cluster treatment, though not environmentally realistic, further aids in teasing apart the
589 nutrient-temperature interactive effects on DA quotas. These LTCN cells were more toxic than the
590 heatwave and extreme heatwave treatments, though not as toxic as the upwelling treatment. Low
591 temperature and pCO_2 are triggers of DA for this strain of *P. australis*, which could partially
592 explain the increased toxicity relative to the heatwave treatments. However, growth rates for the
593 LTCN treatment were lower. Therefore, if all of the available nitrogen was not used for growth in
594 this treatment, there may have been enough left over for DA synthesis. Furthermore, both the
595 upwelling and LTCN treatments efficiently used the available nitrate to support carbon fixation,
596 as NUEs were similar. This indicates that temperature does indeed affect the ability of *P. australis*
597 to use nutrients and synthesize DA.
598
599 Results from the N:P ratio experiments also demonstrate this temperature-nutrient interaction.
600 While growth rates changed minimally across the N:P=50 treatments, there were significant
601 differences in DA quotas within each temperature. This indicates a decoupling between growth
602 rates and DA biosynthesis. Furthermore, when total nutrient concentrations were low, warming
603 constrained DA quotas, yet under high total nutrient concentrations differences in DA quotas were
604 not considerable. This suggests that temperature is more influential on DA quotas when total
605 nutrient concentrations are high. Consequently, under these high total nutrient conditions with
606 excess nitrogen (relative to phosphorus), cells can both double their population size approximately
607 once per day and produce substantial DA, generating a large toxic bloom.

608

609 4.3 Cluster experiments: a holistic view and ecosystem implications

610 Examining the data empirically using cluster experiments can provide a holistic view of how *P.*
611 *australis* bloom formation and toxicity may be impacted by complex events like upwelling and
612 marine heatwaves. In the present study's simulated upwelling and heatwave conditions, similarly
613 high growth rates for both treatments indicate that both conditions could be triggers for bloom
614 formation. These results are consistent with what has been observed in the natural environment:
615 blooms occurring during both upwelling and marine heatwave events (Schnetzer et al. 2013;
616 McCabe et al. 2016; McKibben et al. 2017; Smith et al. 2018). With more frequent heatwave and
617 upwelling events expected as climate change progresses, rapid bloom-forming growth may be
618 triggered more frequently (Bakun et al. 2015). However, if extreme heatwaves exceed the broad
619 thermal optimum for *P. australis* growth, climate change may impede bloom formation. Therefore,
620 the severity of future heatwaves will determine whether *P. australis* will be able to rapidly grow.

621

622 Despite similar growth rates between upwelling and heatwave treatments, only the upwelling
623 conditions led to substantial DA biosynthesis. This suggests that blooms triggered by upwelling
624 may be more toxic than blooms occurring during a heatwave or extreme heatwave event.
625 Furthermore, DA production rates were only substantial in the upwelling treatment. This parameter
626 combines growth rates and toxin quotas to estimate the impact of the bloom (Kelly et al. 2021). A
627 high DA production rate suggests that upwelling events may promote both rapid increases in
628 population size and high concentrations of toxins per cell. Therefore, *P. australis* may be able to
629 form a large, toxic bloom rapidly under these conditions, supporting predictions that blooms will
630 worsen with climate change (Fu et al. 2012; Smith et al. 2018; Gobler 2020; Trainer et al. 2020).

631 Consequentially, blooms triggered by upwelling may be especially harmful to the marine
632 ecosystem, with severe implications for the coastal California system. More frequent, highly toxic
633 blooms could have devastating consequences for ecosystem health and fisheries (McCabe et al.
634 2016). However, in the present experiment pDA quotas normalized to volume were very low
635 compared to maximum concentrations of pDA observed during the Blob bloom (McCabe et al.
636 2016). These values are also well below the regulatory limit for DA (20 ppm). Additionally, DA
637 quotas normalized to cell abundance were a few orders of magnitude lower than a highly toxic *P.*
638 *australis* bloom triggered by upwelling in 2006 (Schnetzer et al., 2013). Therefore, the risk of
639 trophic transfer of domoic acid may not be high for this strain of *P. australis* under upwelling
640 conditions.
641
642 In contrast, although cells in the heatwave treatment grew faster, DA was not detected and thus
643 DA production rates were inconsequential. *P. australis* in the extreme heatwave treatment had
644 neither high growth rates nor high DA quotas. This indicates that despite the ability of *P. australis*
645 to multiply rapidly and form a bloom, toxin production may not be triggered by heatwave
646 conditions. The rapid growth of *Pseudo-nitzschia* spp. under heatwave conditions was also
647 observed during the Blob bloom, with cells persisting in the warm waters, reducing nutrient
648 concentrations in the surface layer of these stratified waters (McCabe et al. 2016). Similar to our
649 experiment, the large population of cells in the northern region of the California Current System
650 did not produce toxins without the availability of nitrogen. However, upwelling occurred in the
651 spring of 2015, fueling the eastern edge of the Blob with nutrients, including nitrogen, which likely
652 allowed the *Pseudo-nitzschia* spp. present to produce DA (McCabe et al. 2016). These seed
653 populations of highly abundant and persistent *Pseudo-nitzschia* sp. populations, triggered by

warming, pose a looming threat ecosystem health, as their toxicity may be triggered by episodic nitrogen inputs. Though our study did not mimic both the heatwave and upwelling aspects of the Blob bloom, future studies should consider heatwave conditions along with a pulse of nutrients.

In contrast, Ryan et al. (2017) found that in Monterey Bay, the high *Pseudo-nitzschia* cell abundance and toxicity was not due the warming anomaly (as temperatures were near normal), but instead correlated with the cold water, upwelling phases. Similarly, Barron et al. (2013) found no correlation between *P. australis* presence in the sediment record and warm anomalies in the Santa Barbara Channel. These studies in the Southern Portion of the California Current System contrast studies that occurred in the Northern portion of the California Current System (McCabe et al. 2016, McKibben et al. 2017). Furthermore, Sandoval-Belmar et al. (2023) found that toxic *Pseudo-nitzschia* blooms in Northern California have been associated with the warm phases of ENSO and PDO, while blooms in Southern California were associated with the cool phases. The strain of *P. australis* used in the present study was isolated from the Northern California Current System (Washington State) and thrived under heatwave conditions. This indicates that regional differences exist regarding the ability of heatwaves to trigger bloom formation.

On the other hand, although heatwaves may trigger a lot of growth, those cells are not expected to be notably toxic without nitrogen input from simultaneous upwelling or an anthropogenic source. While high nutrient concentrations occur in the natural environment during upwelling, dissolved N:P ratios of this water are typically slightly below the Redfield Ratio (N:P= ~12; Feely et al. 2008; Schnetzer et al. 2013; Siedlecki et al. 2016; Larkin et al. 2020). However, increased flow of anthropogenic nitrogen from land to sea (fertilizers and wastewater treatment facility discharge)

677 may increase the N:P ratio of coastal surface waters (Howard et al. 2014). Increased growth and
678 DA quotas in the N:P=50 treatments of the temperature-nutrient matrix experiment suggest that
679 upwelling combined with anthropogenic nutrient inputs might trigger especially toxic *P. australis*
680 blooms, more than upwelling alone. If anthropogenic nutrient inputs occurred during a heatwave,
681 a highly toxic bloom could be triggered due to the excess nitrogen, relative to phosphorus.
682 Furthermore, considerable species and strain specificity exists with regard to the ability of *Pseudo-*
683 *nitzschia* to utilize different nitrogen sources for growth and toxin production (Howard et al. 2007;
684 Kudela et al. 2008; Thessen et al. 2009). Therefore, it is possible that DA biosynthesis for this
685 strain of *P. australis* is not optimized for nitrate, and other sources of nitrogen (e.g., urea and
686 ammonia) should be tested with this strain in the future to further explore the implications of
687 anthropogenic nutrient inputs and their potential interactions with bloom formation and toxicity.
688

689 **5. Conclusions**

690 This study is among the few to examine unialgal *Pseudo-nitzschia* cultures in a multiple driver
691 context, and the first to examine both upwelling and heatwave scenarios in holistic laboratory
692 cluster experiments. These experiments are important for improving our understanding of *P.*
693 *australis* specific responses to these conditions in order to make better predictions about future
694 bloom dynamics in the California Current System. Furthermore, the single factor experiments here
695 provided a unique mechanistic understanding of specific triggers of toxicity and bloom formation
696 for this strain of *P. australis*. This has the potential to improve our ability to predict the occurrence
697 of toxic blooms in the natural environment.
698

699 This experiment only examined one strain of *Pseudo-nitzschia australis*, and these responses may
700 be strain specific. Similar experiments should be conducted with different species and strains
701 isolated from different areas in the California Current System. Furthermore, while we chose to
702 focus on only temperature, nutrients, and pCO_2, the clusters are not truly complete without other
703 factors that have been shown to impact domoic acid synthesis, including biological factors like
704 grazing, competition with other phytoplankton, and the presence of associated bacteria and fungi.
705 Other physical and chemical factors like light intensity and quality, iron concentration, and
706 alternative nitrogen sources are also clearly important (Howard et al. 2007; Thessen et al. 2009;
707 Lelong et al. 2012; Bates et al. 2018; Radan and Cochlan 2018). Considering these factors as well
708 could make these experiments more realistic. Nevertheless, these cluster experiments provide a
709 valuable start towards obtaining a more holistic picture of *P. australis* dynamics during these
710 contrasting events in the future rapidly changing coastal ocean.
711
712 **Acknowledgements**
713 The authors would like to thank Vera Trainer and Brian Bill for isolating and maintaining the
714 *Pseudo-nitzschia australis* strain used in these experiments. We also thank Will Berelson and Nick
715 Rollins for their assistance in running DIC samples.
716
717 **Funding Sources**
718 This work was supported by National Science Foundation award OCE 2120619 to F-XF, and by
719 California Ocean Protection Counsel Proposition 84 funding administered by California Urban
720 Ocean Sea Grant to DAH and FX-F. Funding supporting the LC-MS analysis came from an RI
721 Sea Grant award (NA18OAR4170094) to MB and BJ. The spectrometric measurements were

made in the URI RI-INBRE Centralized Research Core Facility, supported by the Institutional Development Award (IDeA) Network for Biomedical Research Excellence from the National Institute of General Medical Sciences of the National Institutes of Health (P20GM103430).

Author Contributions

F-XF, KJK, and DAH conceived of and designed the experiments with help from BDJ and MJB. F-XF, KK, AM, and CL carried out and sampled the experiments. Subsequent sample processing was done by AM, KK, and F-XF. MJB, AMK, and LAM performed domoic acid extraction and quantification. Data analyses were performed by KK, with help from F-XF and DAH. KK wrote the manuscript with contributions from DAH, F-XF, BDJ, and MJB. All authors reviewed and gave their approval for the final manuscript.

References

Aguilar-Islas, A.M., Bruland, K.W., 2006. Dissolved manganese and silicic acid in the Columbia River plume: A major source to the California current and coastal waters off Washington and Oregon. Mar. Chem. 101(3–4), 233–247.

Auro, M.E., Cochlan, W.P., 2013. Nitrogen utilization and toxin production by two diatoms of the *Pseudo-nitzschia pseudodelicatissima* complex: *P. cuspidata* and *P. fryxelliana*. J. Phycol. 169, 156–169.

Ayache, N., Lundholm, N., Gai, F., Hervé, F., Amzil, Z., Caruana, A., 2021. Impacts of ocean acidification on growth and toxin content of the marine diatoms *Pseudo-nitzschia australis* and *P. fraudulenta*. Mar. Environ. Res. 169, 1-9.

Bakun, A., Black, B.A., Bograd, S.J., García-Reyes, M., Miller, A.J., Rykaczewski, R.R.,

Sydeman, W.J., 2015. Anticipated Effects of Climate Change on Coastal Upwelling Ecosystems. Curr. Clim. Chang. Reports. 1(2), 85–93.

Barron, J.A., Burky, D., Field, D.B., Finney, B., 2013. Response of diatoms and silicoflagellates to climate change and warming in the California Current during the past 250 years and the recent rise of the toxic diatom *Pseudo-nitzschia australis*. Quat. Int. 310, 140-154.

Barth, A., Walter, R.K., Robbins, I., Pasulka, A., 2020. Seasonal and interannual variability of phytoplankton abundance and community composition on the Central Coast of California. Mar. Ecol. Prog. Ser. 637, 29–43.

Bates, S.S., de Freitas, A.S., Milley, J.E., Pocklington, R., Quillam, M.A., Smith, J.C., Worms, J., 1991. Controls on domoic acid production by the diatom *Nitzschia pungens f. multiseries* in culture: nutrients and irradiance. Can. J. Fish. Aquat. Sci. 48,1136–1144.

Bates, S.S., Hubbard, K.A., Lundholm, N., Montresor, M., 2018. *Pseudo-nitzschia, Nitzschia*, and domoic acid: New research since 2011. Harmful Algae. 79, 3-43.

Bif, M.B., Siqueira, L., Hansell, D.A., 2019. Warm Events Induce Loss of Resilience in Organic Carbon Production in the Northeast Pacific Ocean. Global Biogeochem. Cy. 33(9), 1174–1186.

Brzezinski, M.A., Washburn, L., 2011. Phytoplankton primary productivity in the Santa Barbara Channel: Effects of wind-driven upwelling and mesoscale eddies. J. Geophys. Res. Ocean. 116(12), 1-17.

Capone, D.G., Hutchins, D.A., 2013. Microbial biogeochemistry of coastal upwelling regimes in a changing ocean. Nat. Geosci. 6(9), 711–717.

Caron, D.A., Connel, P.E., Schaffner, R.A., Schnetzer, A., Fuhrman, J.A., Countway, P.D., Kim, D.Y., 2017. Planktonic food web structure at a coastal time-series site: I. Partitioning of

768 microbial abundances and carbon biomass. Deep Sea Res. Part I Oceanogr. Res. Pap.
769 121, 14-29.
770 Cavole, L.M., Demko, A.M., Diner, R.E., Giddings, A., Koester, I., Pagniello, C.M.L.S.,
771 Paulsen, M.L., Ramirez-Valdez, A., Schwenck, S.M., Yen, N.K., Zill, M.E., Franks,
772 P.J.S., 2016. Biological impacts of the 2013–2015 warm-water anomaly in the northeast
773 Pacific: Winners, Losers, and the Future. Oceanogr. 29(2), 273–285.
774 Chavez, F.P., Messié, M., 2009. Progress in Oceanography A comparison of Eastern Boundary
775 Upwelling Ecosystems. Prog. Oceanogr. 83(1–4), 80–96.
776 Cheung, W.W.L., Frölicher, T.L., 2020. Marine heatwaves exacerbate climate change impacts
777 for fisheries in the northeast Pacific. Sci. Rep. 10(1), 1–10.
778 Cooley, S.R., Yager, P.L., 2006. Physical and biological contributions to the western tropical
779 North Atlantic Ocean carbon sink formed by the Amazon River plume. J. Geophys. Res.
780 Ocean. 111(8), 1-14.
781 Du, X., Peterson, W.T., 2013. Seasonal Cycle of Phytoplankton Community Composition in the
782 Coastal Upwelling System Off Central Oregon in 2009. Estuaries and Coasts. 37(2), 299–
783 311.
784 Du, X., Peterson, W.T., 2018. Phytoplankton Community Structure in 2011–2013 Compared to
785 the Extratropical Warming Event of 2014–2015. Geophys. Res. Lett. 45(3), 1534–1540.
786 Feely, R.A., Sabine, C.L., Hernandez-Ayon, J.M., Ianson, D., Hales, B., 2008. Evidence for
787 upwelling of corrosive “acidified” water onto the continental shelf. Science. 320(5882),
788 1490–1492.
789 Fehling, J., Davidson, K., Bolch, C.J., Bates, S.S., 2004. Growth and domoic acid production by
790 *Pseudo-nitzschia seriata* (Bacillariophyceae) under phosphate and silicate limitation. J.

Phycol. 40(4), 674–683.

Fu, F.-X., Zhang, Y., Feng, Y., Hutchins, D.A., 2007. Phosphate and ATP uptake and growth kinetics in axenic cultures of the cyanobacterium *Synechococcus* CCMP 1334. Eur. J. Phycol. 41, 15–28.

Fu, F.-X., Mulholland, M.R., Garcia, N.S., Beck, A., Bernhardt, P.W., Warner, M.E., Hutchins, D.A., 2008. Interactions between changing pCO_2, N_2 fixation, and Fe limitation in the marine unicellular cyanobacterium *Crocosphaera*. 53(6), 2472–2484.

Fu, F.-X., Tatters, A.O., Hutchins, D.A., 2012. Global change and the future of harmful algal blooms in the ocean. Mar. Ecol. Pr. 470, 207–233.

Gentemann, C.L., Fewings, M.R., García-Reyes, M., 2017. Satellite sea surface temperatures along the West Coast of the United States during the 2014–2016 northeast Pacific marine heat wave. Geophys. Res. Lett. 44(1), 312–319.

Giordano, M., Beardall, J., Raven, J.A.. 2005. CO_2 concentrating mechanisms in algae: Mechanisms, environmental modulation, and evolution. Annu. Rev. Plant Biol. 56, 99–131.

Gobler, C.J., 2020. Climate Change and Harmful Algal Blooms: Insights and perspective. Harmful Algae. 91, 1–4.

Gómez-Ocampo, E., Gaxiola-Castro, G., Durazo, R., Beier, E., 2018. Effects of the 2013-2016 warm anomalies on the California Current phytoplankton. Deep Sea Res. Part II Top Stud. Oceanogr. 151, 64–76.

Gruber, N., Hauri, C., Lachkar, Z., Loher, D., Frölicher, T.L., Plattner, G., 2012. Rapid Progression of Ocean Acidification in the California Current System. 337(6091), 220-223.

814 Hagström, J.A., Granéli, E., Moreira, M.O.P., Odebrecht, C., 2011. Domoic acid production and
815 elemental composition of two *Pseudo-nitzschia multiseries* strains, from the NW and SW
816 Atlantic Ocean, growing in phosphorus or nitrogen-limited chemostat cultures. J.
817 Plankton Res. 33(2), 297–308.
818 Harðardóttir, S., Hjort, D.M., Wohlrab, S., Krock, B., John, U., Nielsen, T.G., Lundholm, N.,
819 2018. Trophic interactions, toxicokinetics, and detoxification processes in a domoic acid-
820 producing diatom and two copepod species. Limnol. Oceanogr. 64(3), 833-848.
821 Hauri, C., Gruber, N., Plattner, G.-K., Alin, S., Feely, R.A., Hales, B., Wheeler, P.A., 2012.
822 Modeling ocean acidification in the California Current System. Oceanogr. 22(4), 60–71.
823 Howard, M.D.A., Sutula, M., Caron, D.A., Chao, Y., Farrara, J.D., Frenzel, H., Jones, B.,
824 Robertson, G., Mclaughlin, K., Sen Gupta, A., 2014. Anthropogenic nutrient sources
825 rival natural sources on small scales in the coastal waters of the Southern California
826 Bight. Limnol. Oceanogr. 59(1), 285–297
827 Hurd, C.L., Hepburn, C.D., Currie, K.I., Raven, J.A., Hunter, K.A., 2009. Testing the effects of
828 ocean acidification on algal metabolism: Considerations for experimental designs. J
829 Phycol. 45(6), 1236–1251.
830 Hutchins, D.A., Fu, F.-X., 2017. Microorganisms and ocean global change. Nat. Microbiol. 2, 1-
831 11.
832 Jennings, E.D., Parker, M.S., Simenstad, C.A., 2020. Domoic acid depuration by intertidal
833 bivalves fed on toxin-producing *Pseudo-nitzschia multiseries*. Toxicon: X. 6, 1-4.
834 Jiménez-Quiroz, M.dC., Cervantes-Duarte, R., Funes-Rodríguez, R., Barón-Campis, S.A.,
835 García-Romero, F.dJ., Hernández-Trujillo, S., Hernández-Becerril, D.U., González-
836 Armas, R., Martell-Dubois, R., Cerdeira-Estrada, S., Fernández-Méndez, J.I., González-

837 Ania, L.V., Vásquez-Ortiz, M., Barrón-Barraza, F., 2019. Impact of "The Blob" and "El
838 Niño" in the SW Baja California Peninsula: Plankton and environmental variability of
839 Bahia Magdalena. Front. Mar. Sci. 6, 1–23.
840 Kelly, K.J., Fu, F.-X., Jiang, X., Li, H., Xu, D., Yang, N., DeMers, M.A., Kling, J.D., Gao, K.,
841 Ye, N., Hutchins, D.A., 2021. Interactions Between Ultraviolet B Radiation, Warming,
842 and Changing Nitrogen Source May Reduce the Accumulation of Toxic *Pseudo-nitzschia*
843 *multiseries* Biomass in Future Coastal Oceans. Front. Mar. Sci. 8, 1–19.
844 Kling, J.D., Kelly, K.J., Pei, S., Rynearson, T.A., Hutchins, D.A., 2021. Irradiance modulates
845 thermal niche in a previously undescribed low-light and cold-adapted nano-diatom.
846 Limnol. Oceanogr. 66(6), 2266–2277.
847 Lange, C.B., Reid, F.M.H., Vernet, M., 1994. Temporal distribution of the potentially toxic
848 diatom *Pseudonitzschia australis* at a coastal site in Southern California. Mar. Ecol. Prog.
849 Ser. 104, 309–312.
850 Larkin, A.A., Garcia, C.A., Ingoglia, K.A., Garcia, N.S., Baer, S.E., Twining, B.S., Lomas,
851 M.W., Martiny, A.C., 2020. Subtle biogeochemical regimes in the Indian Ocean revealed
852 by spatial and diel frequency of *Prochlorococcus* haplotypes. Limnol. Oceanogr. 65(S1),
853 S220–S232.
854 Lassiter, A.M., Wilkerson, F.P., Dugdale, R.C., Hogue, V.E., 2006. Phytoplankton assemblages
855 in the CoOP-WEST coastal upwelling area. Deep Sea Res. Part II Top Stud. Oceanogr.
856 53(25–26), 3063–3077.
857 Laufkötter, C., Zscheischler, J., Frölicher, T.L., 2020. High-impact marine heatwaves
858 attributable to human-induced global warming. Science. 369(6511), 1621–1625.
859 Lelong, A., Hégaret, H., Soudant, P., Bates, S.S., 2012. *Pseudo-nitzschia* (Bacillariophyceae)

860 species, domoic acid and amnesic shellfish poisoning: revisiting previous paradigms.
861 Phycologica. 51(2), 168–216.
862 Lelong, A., Jolley, D.F., Soudant, P., Hégaret, H., 2012. Impact of copper exposure on *Pseudo-*
863 *nitzschia* spp. physiology and domoic acid production. Aquat. Toxicol. 118–119, 37–47.
864 Lewis, N.I., Bates, S.S., McLachlan, J.L., Smith, J.C., 1993. Temperature effects on growth,
865 domoic acid production and morphology of the diatom *Nitzschia pungens f. multiseries*.
866 In: Smayda, T.J., Shimuzu, Y. (Eds.), Toxic Phytoplankton Blooms in the Sea. Elsevier
867 Sci Publ. B.V., Amsterdam, pp. 601–606.
868 Lewis, E., Wallace, D.W.R., 1998. Program developed for CO_2 system calculations, Carbon
869 Dioxide Information Analysis Center, Report ORNL/CDIAC-105, Oak Ridge
870 National Laboratory, Oak Ridge, Tennessee, USA.
871 Di Lorenzo, E., Mantua, N., 2016. Multi-year persistence of the 2014/15 North Pacific marine
872 heatwave. Nat. Clim. Chang. 6(11), 1042–1047.
873 Lundholm, N., Skov, J., Pocklington, R., Moestrup, O., 1994. Domoic acid, the toxic amino acid
874 responsible for amnesic shellfish poisoning, now in *Pseudonitzschia seriata*
875 (Bacillariophyceae) in Europe. Phycologia. 33(6), 475–478.
876 McCabe, R.M., Hickey, B.M., Kudela, R.M., Lefebvre, K.A., Adams, N.G., Bill, B.D., Gulland,
877 F.M.D., Thomson, R.E., Cochlan, W.P., Trainer, V.L., 2016. An unprecedented
878 coastwide toxic algal bloom linked to anomalous ocean conditions. Geophys. Res. Lett.
879 43(19), 10,366-10,376.
880 McKibben, S.M., Peterson, W., Wood, A.M., Trainer, V.L., Hunter, M., White, A.E., 2017.
881 Climatic regulation of the neurotoxin domoic acid. Proc. Natl. Acad. Sci. 114(2), 239–
882 244.

883 Murata, A., Kumamoto, Y., Saito, C., Kawakami, H., Asanuma, I., Kusakabe, M., Inoue, H.Y.,
884 2002. Impact of a spring phytoplankton bloom on the CO_2 system in the mixed layer of
885 the northwestern North Pacific. Deep Sea Res. Part II Top Stud. Oceanogr. 49(24–25),
886 5531–5555.
887 Oliver, E.C.J., Donat, M.G., Burrows, M.T., Moore, P.J., Smale, D.A., Alexander, L.V.,
888 Benthuysen, J.A., Feng, M., Sen Gupta, A., Hobday, A.J., Holbrook, N.J., Perkins-
889 Kirkpatrick, S.E., Scannell, H.A., Straub, S.C., Wernberg, T. 2018. Longer and more
890 frequent marine heatwaves over the past century. Nat. Commun. 9(1324), 1–12.
891 Pan, Y., Bates, S.S., Cembella, A.D., 1998. Environmental stress and domoic acid production by
892 *Pseudo-nitzschia*: A physiological perspective. Nat. Toxins. 6, 127–135.
893 Pan, Y, Subba Rao, D.V., Mann, K.H., 1996. Changes in domoic acid production and cellular
894 chemical composition of the toxigenic *diatom Pseudo-nitschia multiseries* under
895 phosphate limitation. J. Phycol. 32(3), 371–381
896 Peña, M.A., Nemcek, N., Robert, M., 2019. Phytoplankton responses to the 2014–2016 warming
897 anomaly in the northeast subarctic Pacific Ocean. Limnol. Oceanogr. 64(2), 515–525.
898 Radan, R.L., Cochlan, W.P., 2018. Differential toxin response of *Pseudo-nitzschia multiseries* as
899 a function of nitrogen speciation in batch and continuous cultures, and during a natural
900 assemblage experiment. Harmful Algae. 73, 12–29.
901 Remy, M., Hillebrand, H., Flöder, S., 2017. Stability of marine phytoplankton communities
902 facing stress related to global change: Interactive effects of heat waves and turbidity. J.
903 Exp. Mar. Bio. Ecol. 497, 219–229.
904 Roche, K.M., Sterling, A.R., Rynearson, T.A., Bertin, M.J., Jenkins, B.D., 2022. A Decade of
905 Time Series Sampling Reveals Thermal Variation and Shifts in Pseudo-nitzschia Species

Composition That Contribute to Harmful Algal Blooms in an Eastern US Estuary. Front Mar. Sci. 9, 1–11.

Ryan, J.P., Kudela, R.M., Birch, J.M., Blum, M., Bowers, H.A., Chavez, F.P., Doucette, G.L., Hayashi, K., Marin III, R., Mikulski, C.M., Pennington, J.T., Scholin, C.A., Smith, G.J., Woods, A., Zhang, Y., 2013. Causality of an extreme harmful algal bloom in Monterey Bay, California, during the 2014–2016 northeast Pacific warm anomaly. Geophys. Res. Lett. 44, 5571–5579.

Sandoval-Belmar, M., Smith, J., Moreno, A.R., Anderson, C., Kudela, R.M., Sutula, M., Kessouri, F., Caron, D.A., Chavez, F.P., Bianchi, D., 2023. A cross-regional examination of patterns and environmental drivers of *Pseudo-nitzschia* harmful algal blooms along the California coast. Harmful Algae.

Schnetzer, A., Jones, B.H., Schaffner, R.A., Cetinic, I., Fitzpatrick, E., 2013. Coastal upwelling linked to toxic *Pseudo-nitzschia australis* blooms in Los Angeles coastal waters, 2005 – 2007. 35, 1080–1092.

Schnetzer, A., Jones, B.H., Schaffner, R.A., Cetinic, I., Fitzpatrick, E., Miller, P.E., Seubert, E.L., Caron, D.A., 2013. Coastal upwelling linked to toxic *Pseudo-nitzschia australis* blooms in Los Angeles coastal waters, 2005-2007. J. Plankton Res. 35(5), 1080–1092.

Sen Gupta, A., Thomsen, M., Benthuysen, J.A., Hobday, A.J., Oliver, E., Alexander, L.V., Burrows, M.T., Donat, M.G., Feng, M., Holbrook, N.J., Perkins-Kirkpatrick, S., Moore, P.J., Rodrigues, R.R., Scannell, H.A., Taschetto, A.S., Ummenhofer, C.C., Wernberg, T., Smale, D.A., 2020. Drivers and impacts of the most extreme marine heatwaves events. Sci Rep. 10(1), 1–15.

Siedlecki, S.A., Kaplan, I.C., Hermann, A.J., Nguyen, T.T., Bond, N.A., Newton, J.A., Williams,

G.D., Peterson, W.T., Alin, S.R., Feely, R.A., 2016. Experiments with Seasonal Forecasts of ocean conditions for the Northern region of the California Current upwelling system. Sci. Rep. 6, 1–18.

Smith, J., Connell, P., Evans, R.H., Gellene, A.G., Howard, M.D.A., Jones, B.H., Kaveggia, S., Palmer, L., Schnetzer, A., Seegers, B.N., Seubert, E.L., Tatters, A.O., Caron, D.A., 2018. A decade and a half of *Pseudo-nitzschia* spp. and domoic acid along the coast of southern California. Harmful Algae. 79:87–104.

Soulié, T., Vidussi, F., Mas, S., Mostajir, B., 2022. Functional Stability of a Coastal Mediterranean Plankton Community During an Experimental Marine Heatwave. Front. Mar. Sci. 9, 1-17.

Sterling, A.R., Kirk, R.D., Bertin, M.J., Rynearson, T.A., David, G., Caponi, M.C., Carney, J., Hubbard, K.A., King, M.A., Maranda, L., McDermith, E.J., Santos, N.R., Strock, J.P., Tully, E.M., Vaverka, S.B., Wilson, P.D., Jenkins, B.D., 2022. Emerging harmful algal blooms caused by distinct seasonal assemblages of the toxic diatom. bioRxiv. Limnol. Oceanogr. 67(11), 2341-2359.

Subhas, A.V., Rollins, N.E., Berelson, W.M., Dong, S., Erez, J., Adkins, J.F., 2015. A novel determination of calcite dissolution kinetics in seawater. Geochim. Cosmochim. Acta. 170, 51–68.

Sun, J., Hutchins, D.A., Feng, Y., Seubert, E.L., Caron, D.A., Fu, F.-X., 2011. Effects of changing pCO_2 and phosphate availability on domoic acid production and physiology of the marine harmful bloom diatom *Pseudo-nitzschia multiseries*. Limnol. Oceanogr. 56(3), 829–840.

Tatters, A.O., Fu, F.-X., Hutchins, D.A., 2012. High CO_2 and silicate limitation synergistically

952 increase the toxicity of *Pseudo-nitzschia fraudulenta*. PLoS One. 7(2), 1-7.
953 Tatters, A.O., Schnetzer, A., Xu, K., Walworth, N.G., Fu, F.-X., Spackeen, J.L., Sipler, R.E.,
954 Bertrand, E.M., McQuaid, J.B., Allen, A.E., Bronk, D.A., Gao, K., Sun, J., Caron, D.A.,
955 Hutchins, D.A., 2018. Interactive effects of temperature, CO_2 and nitrogen source on a
956 coastal California diatom assemblage. J. Plankton Res. 40(2), 151-164.
957 Thorel, M., Fauchot, J., Morelle, J., Raimbault, V., Le Roy, B., Miossec, C., Kientz-Bouchart,
958 V., Claquin, P., 2014. Interactive effects of irradiance and temperature on growth and
959 domoic acid production of the toxic diatom *Pseudo-nitzschia australis*
960 (Bacillariophyceae). Harmful Algae. 39, 232-241.
961 Trainer, V.L., Adams, N.G., Bill, B.D., Stehr, C.M., Wekell, J.C., Moeller, P., Busman, M.,
962 Woodruff, D., 2000. Domoic acid production near California coastal upwelling zones,
963 June 1998. Limnol. Oceanogr. 45(8), 1818–1833.
964 Trainer, V.L., Bates, S.S., Lundholm, N., Thessen, A.E., Cochlan, W.P., Adams, N.G., Trick,
965 C.G., 2012. *Pseudo-nitzschia* physiological ecology, phylogeny, toxicity, monitoring and
966 impacts on ecosystem health *Pseudo-nitzschia* physiological ecology, phylogeny,
967 toxicity, monitoring and impacts on ecosystem health. Harmful Algae. 14, 271–300.
968 Trainer, V.L., Kudela, R.M., Hunter, M.V., Adams, N.G., McCabe, R.M., 2020. Climate
969 Extreme Seeds a New Domoic Acid Hotspot on the US West Coast. Front. Clim. 2, 1–11.
970 Wang, Z., Maucher-Fuquay, J., Fire, S.E., Mikulski, C.M., Haynes, B., Doucette, G.J., Ramsdell,
971 J.S. 2012. Optimization of solid-phase extraction and liquid chromatography-tandem
972 mass spectrometry for the determination of domoic acid in seawater, phytoplankton, and
973 mammalian fluids and tissues. Anal. Chim. Acta 715, 71-79.
974 Welschmeyer, N.A., 1994. Fluorometric analysis of chlorophyll a in the presence of chlorophyll

b and pheopigments. Limnol. Oceanogr. 39(8), 1985–1992.

Wingert, C.J., Cochlan, W.P., 2021. Effects of ocean acidification on the growth, photosynthetic performance, and domoic acid production of the diatom *Pseudo-nitzschia australis* from the California Current System. Harmful Algae. 107, 1-18.

Yang, B., Emerson, S.R., Angelica, Penã ,M., 2018. The effect of the 2013-2016 high temperature anomaly in the subarctic Northeast Pacific (the "blob") on net community production. Biogeosciences. 15(21), 6747–6759.

Yang, N., Lin, Y.A., Merkel, C.A., DeMers, M.A., Qu, P.P., Webb, E.A., Fu, F.-X., Hutchins, D.A., 2022. Molecular mechanisms underlying iron and phosphorus co-limitation responses in the nitrogen-fixing cyanobacterium *Crocosphaera*. ISME J. 16, 2702-2711.

Zhu, Z., Qu, P., Fu, F.-X., Tennenbaum, N., Tatters, A.O., Hutchins, D.A., 2017. Understanding the blob bloom: Warming increases toxicity and abundance of the harmful bloom diatom *Pseudo-nitzschia* in California coastal waters. Harmful Algae. 67, 36–43.

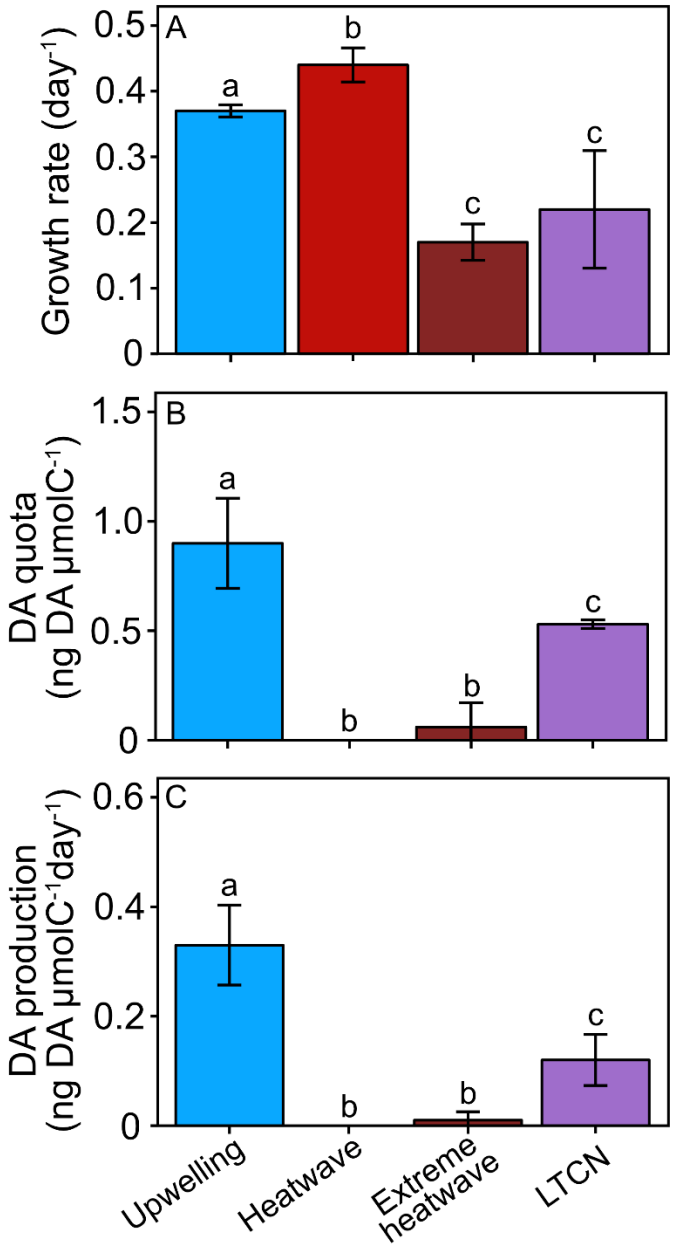

989

990 **Figure 1.** Average growth rates (a), particulate domoic acid quotas (b), and domoic acid
991 production rates for scenario experiments with combined CO_2, temperature, and nutrients
992 representative of upwelling, heatwaves, extreme heatwave, and low temperature, CO_2, and
993 nutrients (LTCN) conditions. Different letters indicate that differences between treatments are
994 statistically significant, while the same letters indicate that differences between treatments are not
995 statistically significant. Error bars represent standard deviation of the mean.

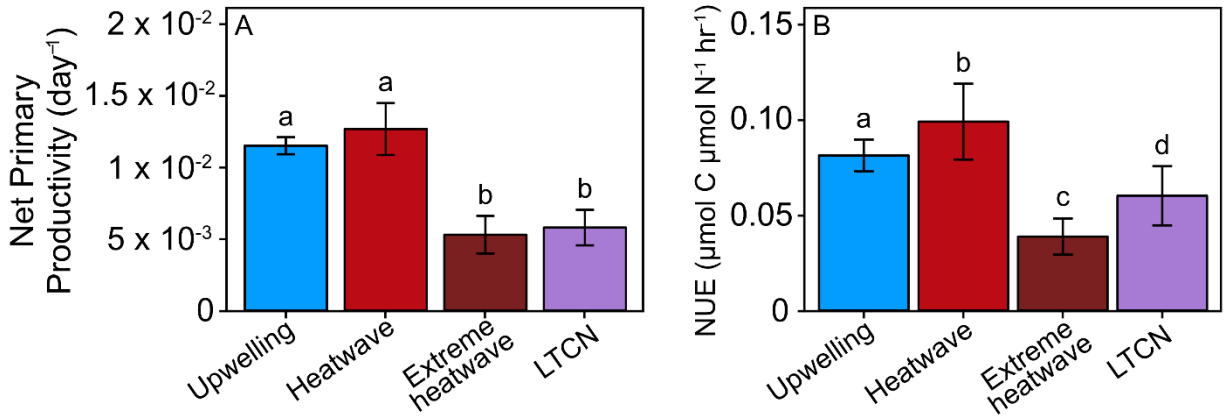

996

997 **Figure 2.** Net primary productivity (A), nitrogen use efficiency (NUE; B) of *P. australis* under
998 upwelling, LTCN, heatwave, and extreme heatwave conditions. Different letters indicate that
999 differences between treatments are statistically significant, while the same letters indicate that
1000 differences between treatments are not statistically significant. Error bars represent standard
1001 deviation of the mean.

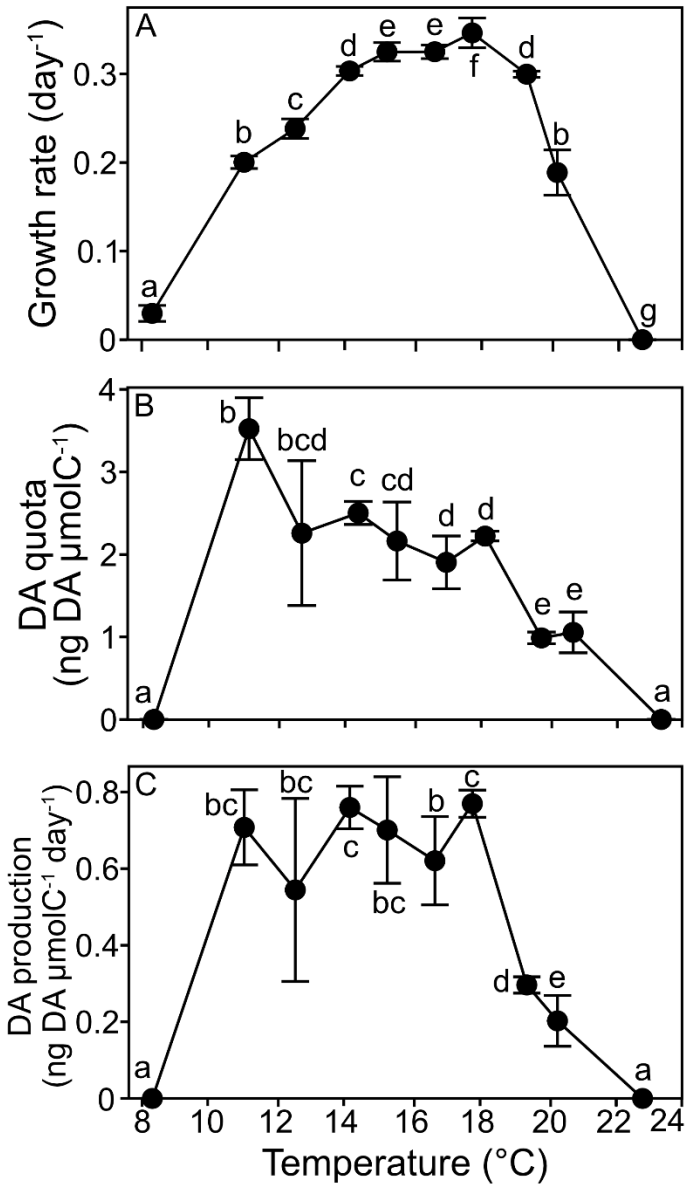

1002

1003 **Figure 3.** N Average *P. australis* growth rates (A), particulate domoic acid (pDA) cellular quotas

1004 (ng DA µmol C^{-1}) (B), and domoic acid production rates (ng DA µmol C^{-1} d^{-1}) (C) across a range

1005 of temperatures. Different letters indicate different statistically significant differences between

1006 temperatures, and error bars represent standard deviations of the mean (n=3).

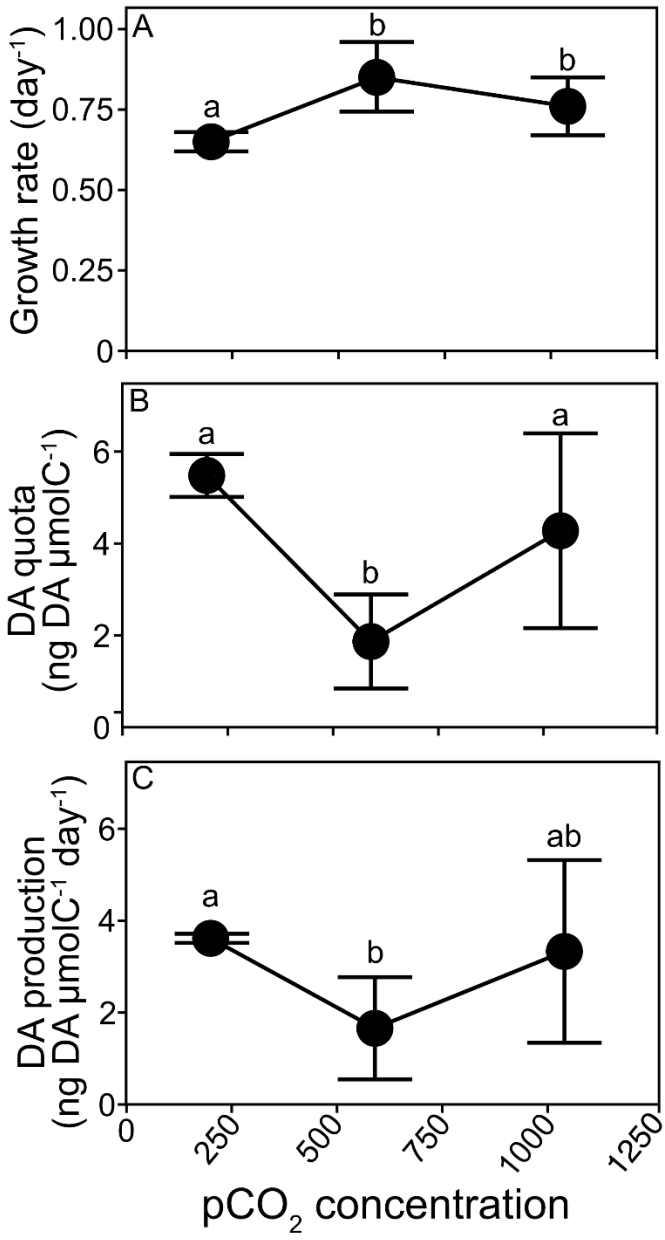

Figure 4. Growth rates (A), particulate domoic acid concentrations (B), and domoic acid production rates (C) measured in the single factor pCO_2 experiments. Different letters indicate statistically significant differences between temperatures, and error bars represent standard deviations of the mean.

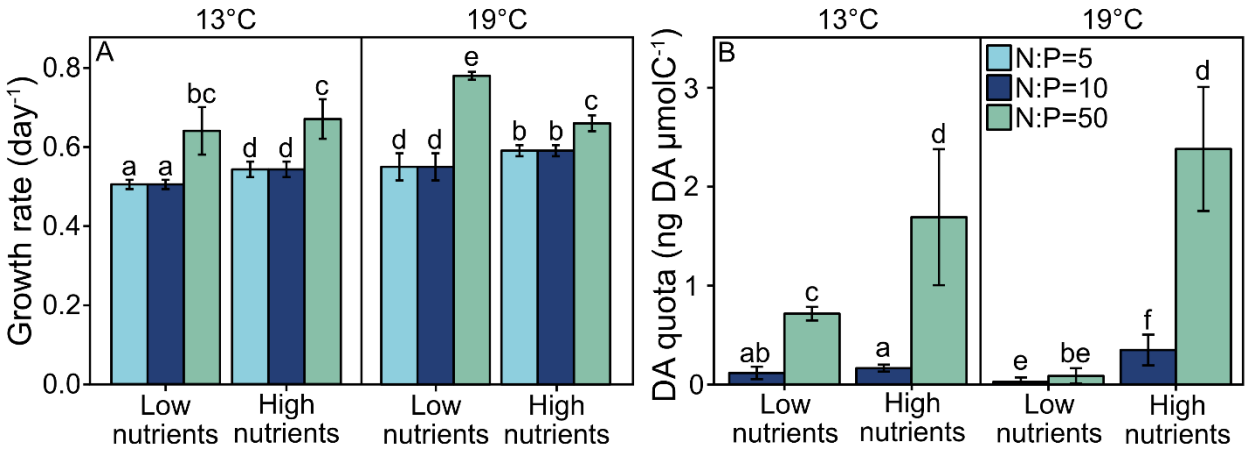

1012

1013 **Figure 5.** Specific growth rates for all N:P ratio experiments (A) and particulate domoic acid
1014 quotas for the N:P=10 and N:P=50 experiments (B). Domoic acid was not detected in the N:P=5
1015 experiments. Different letters indicate different statistically significant differences between
1016 temperatures, and error bars represent standard deviations of the mean.

1017

Table 1: Levels of treatment for cluster experiments, with altered temperature, pCO_2, and nutrients[1].

Treatment	Upwelling	LTCN	Heatwave	Extreme heatwave
Temperature	13°C	13°C	19°C	20.5°C
pCO_2	900 µatm	230 µatm	255 µatm	240 µatm
Nutrients	3 µM PO_4 40 µM $Si(OH)_4$ 30 µM NO_3	0.5 µM PO_4 10 µM $Si(OH)_4$ 5 µM NO_3	0.5 µM PO_4 10 µM $Si(OH)_4$ 5 µM NO_3	0.5 µM PO_4 10 µM $Si(OH)_4$ 5 µM NO_3

[1] LTCN = low temperature, carbon dioxide, and nutrients.

Table 2: Experimental treatments in the nutrient-temperature matrix experiment. Each treatment below was grown under two temperature conditions: 13 and 19°C.

N:P ratio	Total nutrient concentration	Nitrate (µM)	Phosphate (µM)	Silicate (µM)
5	Low	5	1	10
	High	30	6	40
10	Low	5	0.5	10
	High	30	3	40
50	Low	5	0.1	10
	High	30	0.6	40

Table 3: Calculated carbonate buffer system based on pH and DIC measurements. Values in parentheses represent the standard deviation of the mean[2].

		Measured pH	Measured DIC (µmol/kg)	Calculated bulk alkalinity (µmol/kg)	Calculated pCO_2 (µatm)
Cluster experiments	**Upwelling**	7.7 (0.01)	2098.0 (17.8)	32.9 (0.7)	889.1 (29.0)
	LTCN	8.2 (0.01)	1868 (16.9)	90.1 (0.8)	229.3 (4.6)
	Heatwave	8.24 (0.02)	1785 (4.6)	93.5 (2.5)	254.3 (9.4)
	Extreme heatwave	8.24 (0.04)	1787.1 (24.8)	95.2 (3.9)	240.2 (23.2)
Single-factor experiments	**Pre-industrial**	8.29 (0.08)	1884 (23.2)	117.7 (14.6)	201.8 (36.5)
	Ocean acidification	7.89 (0.01)	2058 (13.1)	53.5 (1.1)	592.2 (14.3)
	Extreme ocean acidification	7.68 (0.01)	2166 (26.2)	34.4 (0.5)	1038.9 (4.7)

[2]LTCN = low temperature, carbon dioxide, and nutrients.

1028 Table 4: Average domoic acid (DA) quotas for the cluster experiment, normalized to cell
1029 abundance.

Treatment	Average ng DA/cell (standard deviation)	Average ng DA/mL (standard deviation)
Upwelling	7×10^{-5} (4.3×10^{-5})	0.07 (0.01)
Heatwave	0 (0)	0 (0)
Extreme heatwave	6.9×10^{-6} (1.2×10^{-5})	0.01 (0.01)
LTCN	2.61×10^{-5} (8.65×10^{-6})	0.04 (0.04)

1030